

Mechanistic insights into the pseudocapacitive performance of bronze-type vanadium dioxide with mono/multi-valent cations intercalation

Ying Zeng^{1#}, Jian Hu^{1, 2#}, Jiaofeng Yang³, Pei Tang¹, Qingfeng Fu¹, Wang Zhou¹, Yufan Peng¹,
Peitao Xiao⁴, Shi Chen⁵, Kunkun Guo¹, Peng Gao^{1*}, Hongliang Dong^{6,7*}, and Jilei Liu^{1*}

¹College of Materials Science and Engineering, Hunan Joint International Laboratory of Advanced Materials and Technology for Clean Energy, Hunan Province Key Laboratory for Advanced Carbon Materials and Applied Technology, Hunan University, Changsha 410082, China

²Hunan Provincial Key Laboratory of Fine Ceramics and Powder Materials, School of Materials and Environmental Engineering, Hunan University of Humanities, Science and Technology, Loudi, Hunan 417000, China

³Hunan Communications Research Institute Co. Ltd., Changsha 410015, China

⁴Department of Materials Science and Engineering, National University of Defense Technology, Changsha, Hunan, 410073, China

⁵Joint Key Laboratory of the Ministry of Education, Institute of Applied Physics and Materials Engineering, University of Macau, Avenida da Universidade, Taipa, Macau 999078, China

⁶Center for High Pressure Science and Technology Advanced Research, Pudong, Shanghai 201203, China

⁷State Key Laboratory of High Performance Ceramics and Superfine Microstructure, Shanghai Institute of Ceramics, Chinese Academy of Sciences, Shanghai 201899, China

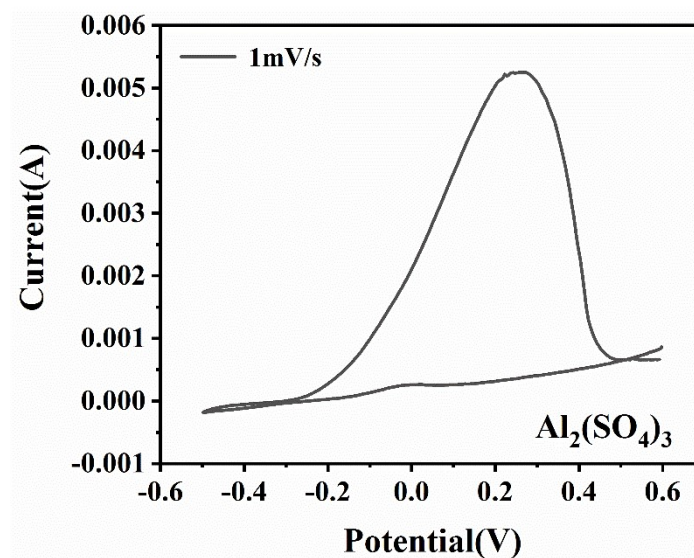


Fig. S1 Cyclic voltammetry curve of VO₂(B) cycled in 1 M Al₂(SO₄)₃ electrolyte measured at 1 mV/s scan rate.

Table S1. Solvothermal reaction conditions used to optimize the pseudocapacitive performance of as-synthesized VO₂(B) electrodes.

| Sample No. | 1-0 | 1-1 | 1-2 | 1-3 | 1-4 |
|---------------------------------------|-------|-------|-------|-------|-------|
| Reaction conditions | | | | | |
| Volume ratio of water/ethylene glycol | 3 : 2 | 1 : 1 | 2 : 3 | 3 : 2 | 3 : 2 |
| Reaction time (h) | 6 | 6 | 6 | 7 | 8 |

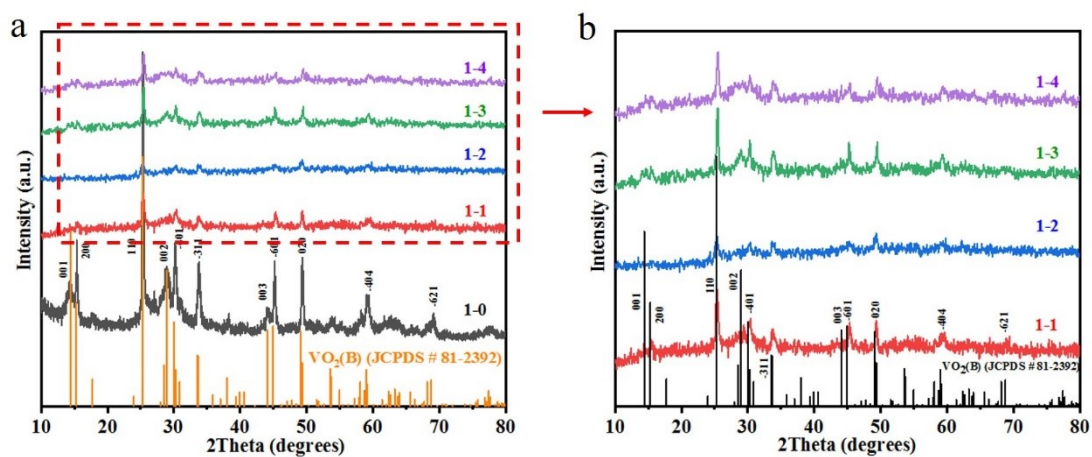


Fig. S2 XRD patterns of vanadium dioxides (Sample 1-0 to 1-4) prepared with different solvothermal reaction conditions.

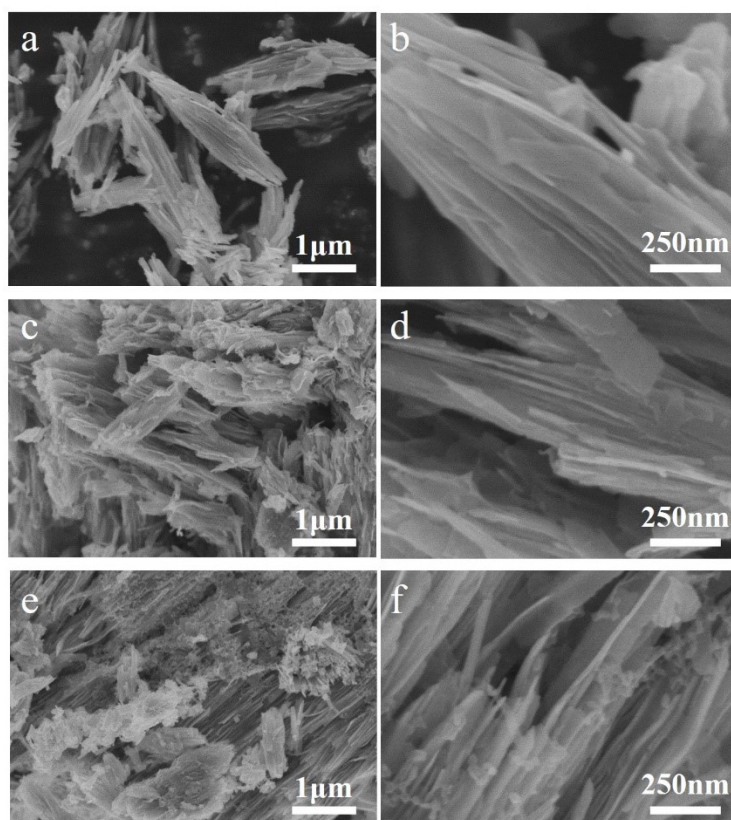


Fig. S3 SEM images of vanadium dioxides (Sample 1-0 to 1-2) prepared with different solvothermal reaction conditions.

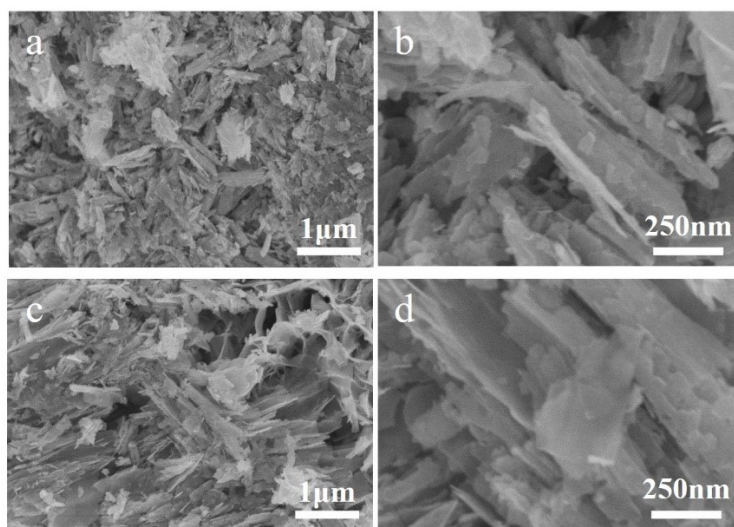


Fig. S4 SEM images of vanadium dioxides (Sample 1-3 to 1-4) prepared with different solvothermal reaction conditions.

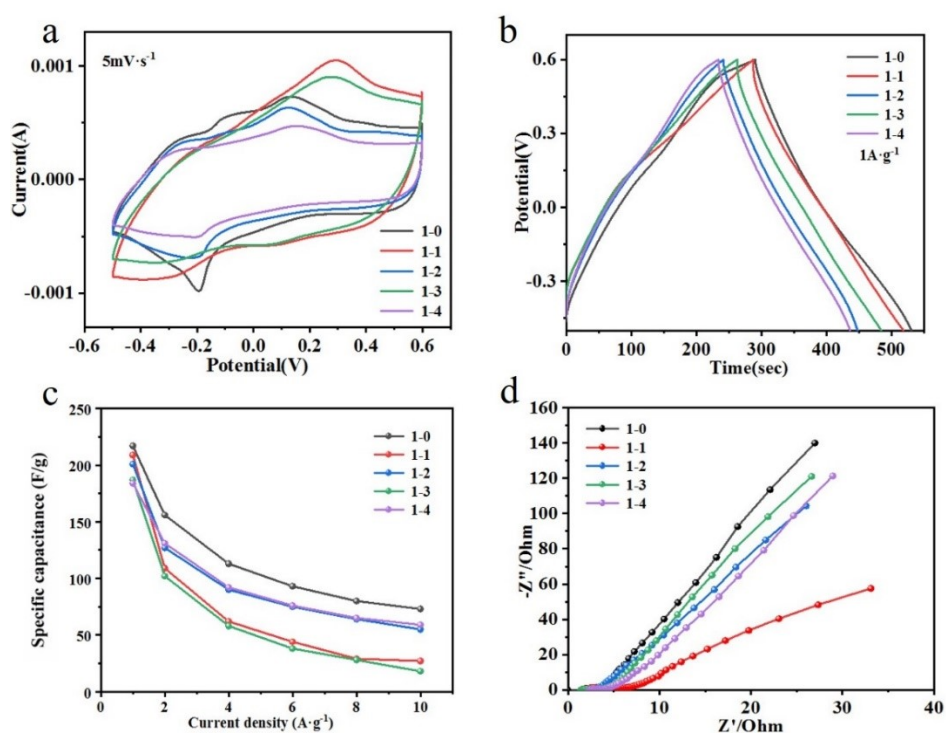


Fig. S5 Electrochemical measurements of vanadium dioxides (Sample 1-0 to 1-4) prepared with different solvothermal reaction conditions. (a) cyclic voltammetry curves measured at 5 mV/s scan rate, (b) galvanostatic charge-discharge curves measured at 1 A/g current density, (c) specific capacitances at various current densities, (d) Nyquist plots.

Table S2. Summary of specific capacitances and rate capabilities of vanadium dioxides (Sample 1-0 to 1-4) prepared with different solvothermal reaction conditions.

| Samples | 1-0 | 1-1 | 1-2 | 1-3 | 1-4 |
|---|-------|-------|-------|-------|-------|
| Specific capacitances (F/g) | 217.6 | 209.8 | 201.0 | 200.7 | 183.3 |
| Capacitance retention with $\times 10$ increased current density (%) | 33.6 | 12.9 | 27.4 | 9.6 | 32.0 |

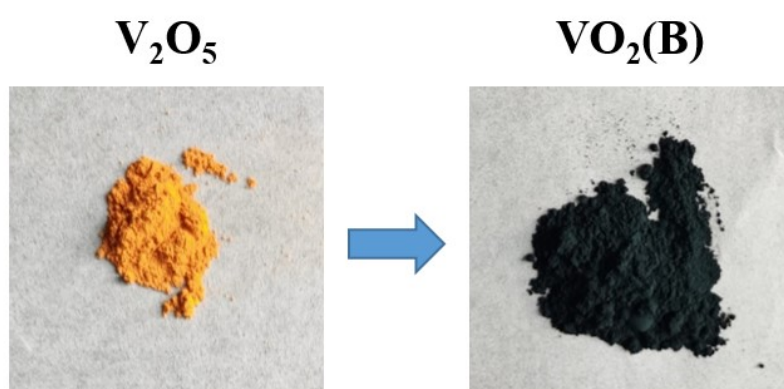


Fig. S6 Color variation from yellow to dark blue after solvothermal reduction reaction indicates the transformation of V_2O_5 to pure phase $VO_2(B)$.

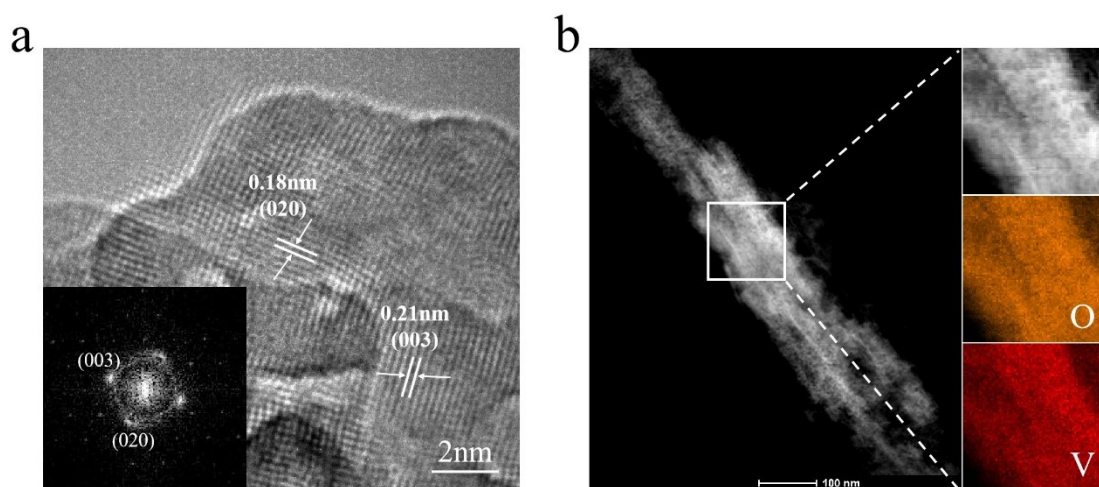


Fig. S7 (a) HRTEM image of $VO_2(B)$ with the corresponding fast Fourier transform (FFT) pattern in the inset, (b) HAADF-STEM image and EDS elemental mapping of V and O.

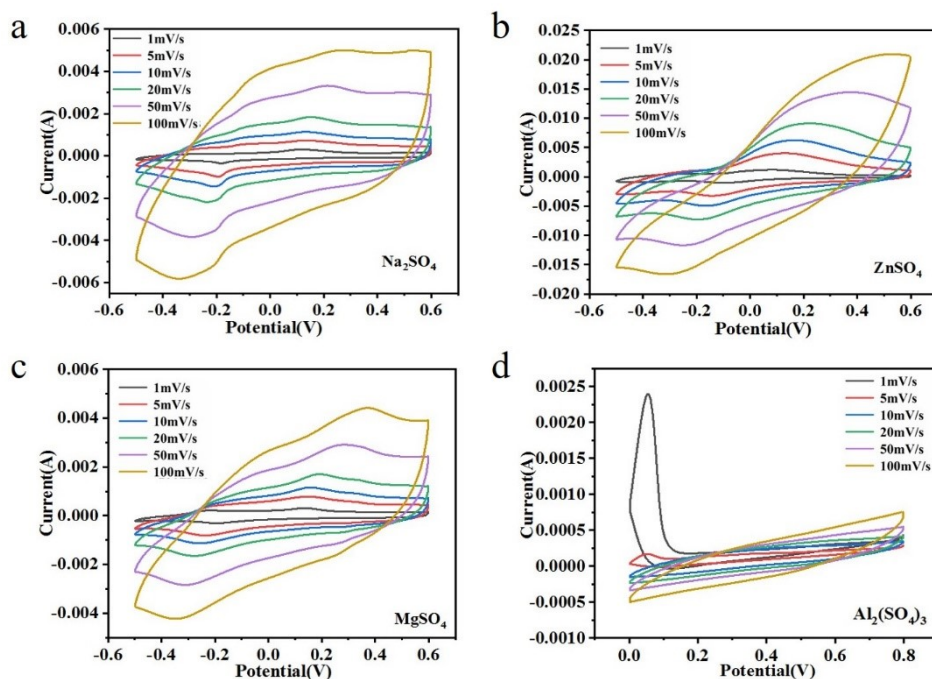


Fig. S8 Cyclic voltammetry curves of $\text{VO}_2(\text{B})$ cycled in Na_2SO_4 , MgSO_4 , ZnSO_4 and $\text{Al}_2(\text{SO}_4)_3$ electrolytes

at various scan rates from 1 to 100 mV/s.

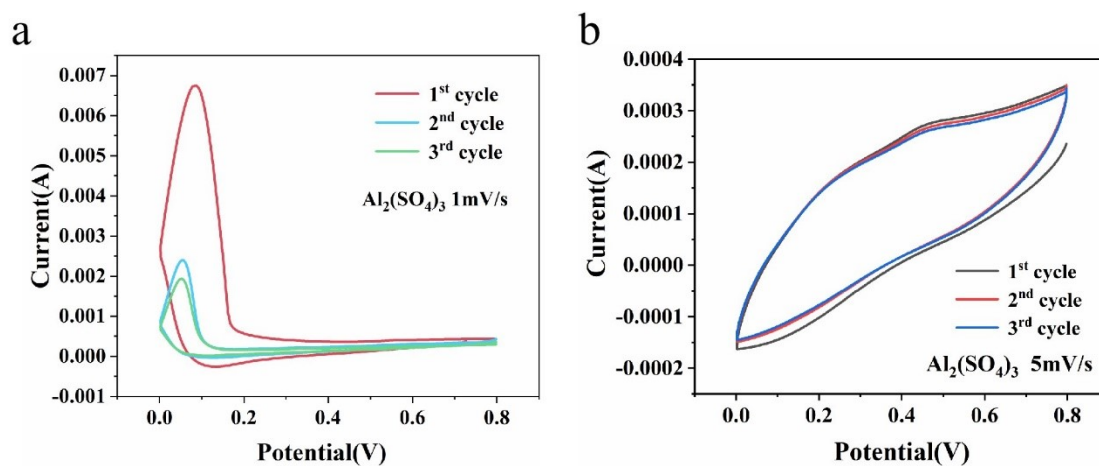


Fig. S9 Cyclic voltammetry curves of $\text{VO}_2(\text{B})$ cycled in $\text{Al}_2(\text{SO}_4)_3$ electrolyte at (a) 1 mV/s and (b) 5 mV/s.

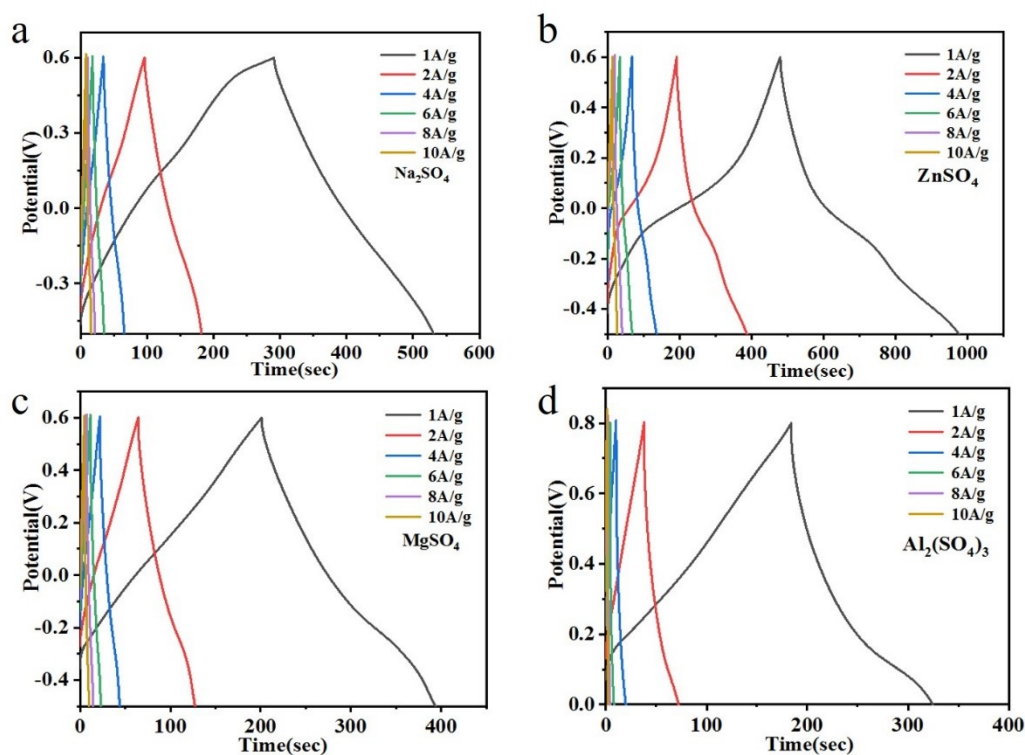


Fig. S10 Galvanostatic charge-discharge curves of $\text{VO}_2(\text{B})$ cycled in Na_2SO_4 , MgSO_4 , ZnSO_4 and $\text{Al}_2(\text{SO}_4)_3$

electrolytes at different current densities from 1 to 10 A/g.

Table S3. Summary of the specific capacitances of $\text{VO}_2(\text{B})$ cycled in Na_2SO_4 , MgSO_4 , ZnSO_4 and

$\text{Al}_2(\text{SO}_4)_3$ electrolytes at different current densities from 1 to 10 A/g.

| Current density (A/g) | Specific capacitance (F/g) | | | |
|--------------------------|----------------------------|------------------|------------------|------------------|
| | Na^+ | Zn^{2+} | Mg^{2+} | Al^{3+} |
| 1 | 218 | 460 | 180 | 151 |
| 2 | 147 | 371 | 120 | 60 |
| 4 | 109 | 274 | 88 | 19 |
| 6 | 89 | 219 | 74 | 11 |
| 8 | 76 | 181 | 65 | |
| 10 | 71 | 158 | 59 | |

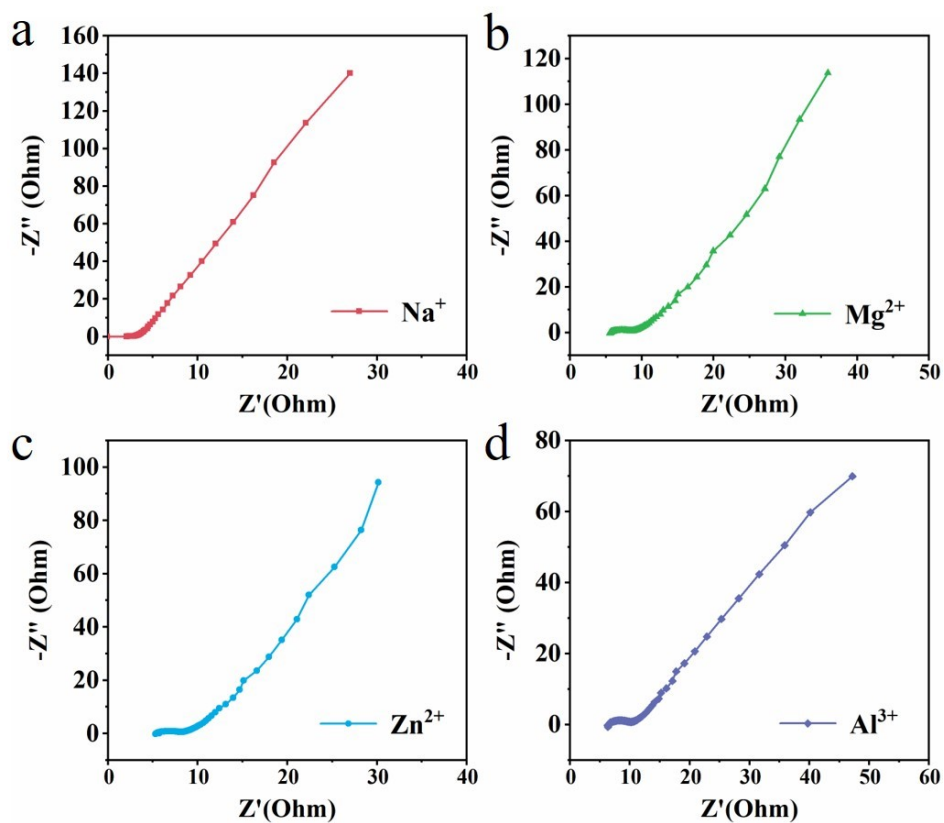


Fig. S11 Nyquist plots of $\text{VO}_2(\text{B})$ cycled in (a) Na_2SO_4 , (b) MgSO_4 , (c) ZnSO_4 and (d) $\text{Al}_2(\text{SO}_4)_3$ electrolytes.

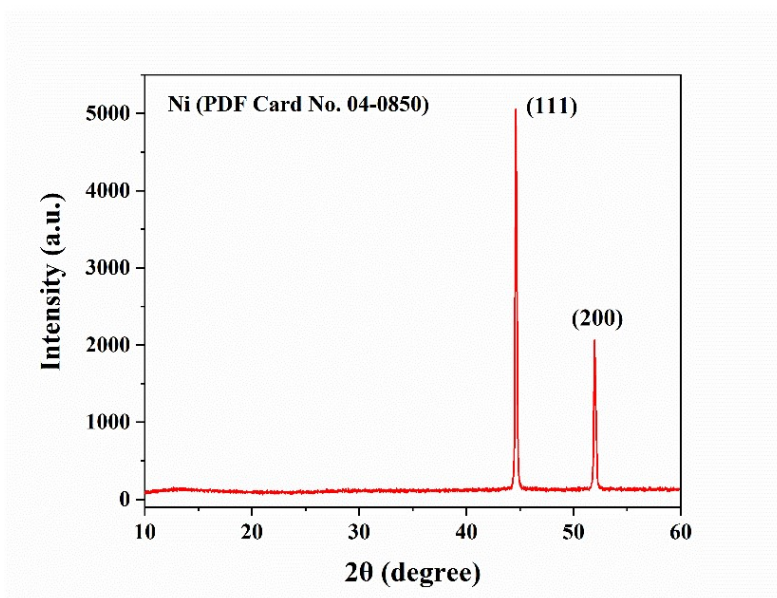


Fig. S12 XRD pattern of the pure nickel foam.

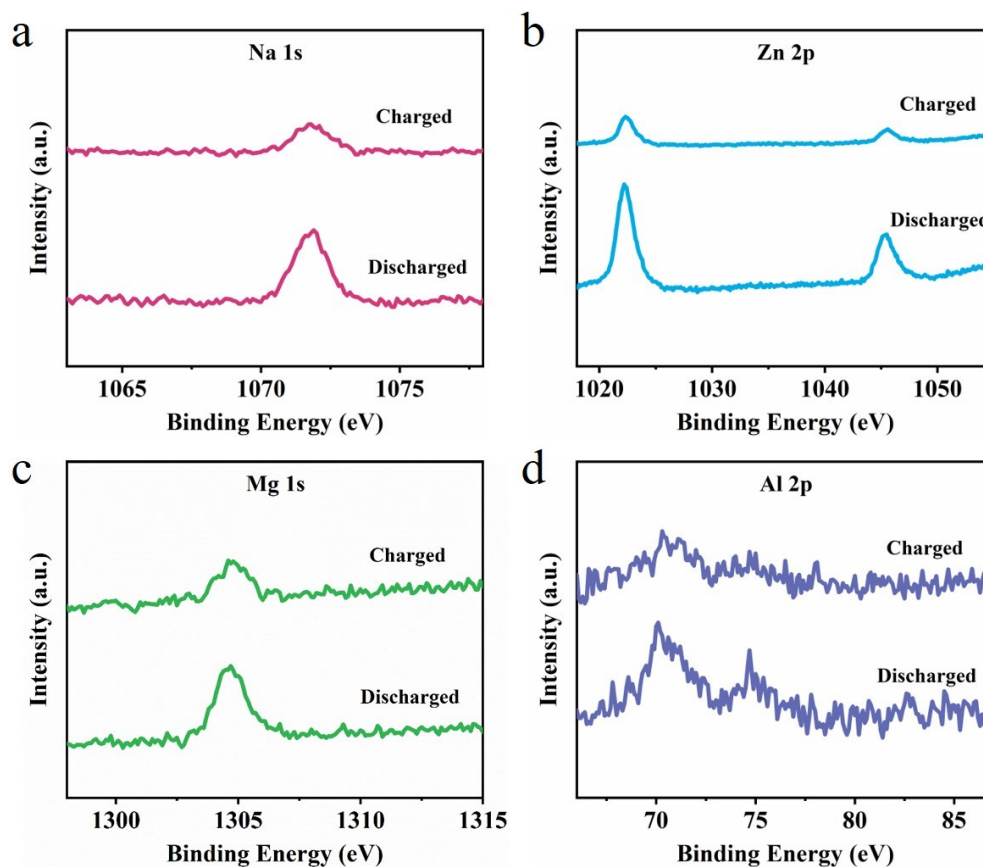


Fig. S13 High-resolution XPS spectra of (a) Na 1s, (b) Zn 2p, (c) Mg 1s, and (d) Al 2p at fully charged and discharged states.

Table S4. Summary of adsorption energy of Na, Mg, Zn and Al on $\text{VO}_2(\text{B})$'s surfaces.

| Electrolyte ions | Na | Mg | Zn | Al |
|------------------------|-------|-------|-------|-------|
| Adsorption energy (eV) | -3.39 | -4.78 | -0.83 | -8.17 |

Table S5. Summary of ΔE_{tol} , ΔE_{zpe} , ΔS and ΔG for standard Gibbs free energy change calculation during the formation process of $\text{Zn}_3(\text{OH})_2\text{V}_2\text{O}_7$.

| ΔE_{tol} | ΔE_{zpe} | ΔS | ΔG |
|-------------------------|-------------------------|-------------|--------------|
| -0.480883325 | -0.267381 | -0.22108313 | -0.527181195 |